THE JOURNAL OF PHYSICAL CHEMISTRY A

Article

pubs.acs.org/JPCA

Temperature and Size Dependence of Characteristic Hydrogen-Bonded Network Structures with Ion Core Switching in Protonated (Methanol)$_{6-10}$−(Water)$_1$ Mixed Clusters: A Revisit

Marusu Katada,[†,‡] Po-Jen Hsu,[§,‡] Asuka Fujii,*[,†] and Jer-Lai Kuo*[,§]

[†]Department of Chemistry, Graduate School of Science, Tohoku University, Sendai 980-8578, Japan

[§]Institute of Atomic and Molecular Sciences, Academia Sinica, Taipei, 10617, Taiwan

Supporting Information

ABSTRACT: Hydrogen-bonded network structures and preferential ion core in the protonated methanol−water mixed clusters, $H^+(methanol)_n-(water)_1$ (n = 6−10), were explored by a combination of infrared spectroscopy and theoretical calculations. Infrared spectra of the OH stretch region of the clusters were measured at the two different temperature ranges by using Ar-tagging. Stable isomer structures of the clusters were searched by the multiscale modeling approach and temperature dependent infrared spectra were simulated based on the statistical populations of the isomers. The combined experimental and theoretical studies revealed that the characteristic multiring structures begin to form at n = 7 under the low temperature condition and they are preferential at the wide temperature range in $n \geq 8$. It was also demonstrated that the preferential ion core type changes from methanol ($MeOH_2^+$) to water (H_3O^+) with increasing cluster size. In $n \leq 8$, the observed infrared spectral features partly depend on the monitoring vibrational predissociation channel, and weak correlations between the hydrogen-bonded network structure and preferential dissociation channels were suggested. However, the ion core type does not necessarily correlate to the preferential dissociation channel. This implies that large rearrangement of the hydrogen-bonded network structure occurs prior to the dissociation.

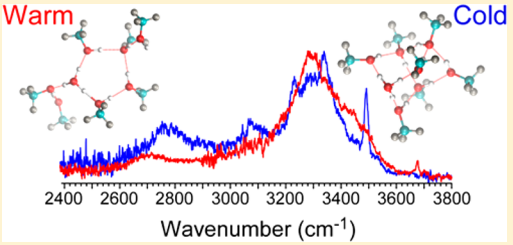

I. INTRODUCTION

Protonated clusters in the gas phase are a model system of proton solvation in the solution.[1−18] Protonated clusters of typical protic solvents, such as water, methanol, and ammonia, have been extensively studied both by theoretical and experimental methods. Their proton solvation motifs and hydrogen-bonded (H-bonded) network structures have attracted great interest. It has been demonstrated that the preferential H-bonded network structure strongly depends on the species of the protonated cluster. For example, the H-bonded networks of protonated water clusters develop from radial tree structures to three-dimensional cage structures as the size increases.[1−6,19−21] On the other hand, protonated methanol clusters form much simpler (bi)cyclic or linear chain structures even in large sizes.[7−11,22−26] An origin of such a difference in the structure development process is obviously the H-bond coordination property of the species, which determines the topological property of the H-bonded networks.[6,7,19,20,22−24,27−33] This means that if molecules of different H-bond coordination properties are mixed, H-bonded network structures of the mixed system can be different both from the single component systems.

In a protonated binary mixed cluster, not only its H-bonded network structures but also the preferential location of the excess proton (protonated site) is of great interest.[1,15−18,34] In a naive idea, the preferential protonated site should be the component of the larger proton affinity (PA). In the last 2 decades, however, there have been many reports on the preferential protonation to the smaller PA site in mixed clusters.[35−38] Then, it has been established that solvation energy of the protonated site is also important in determination of the preferential protonation site. This means that the preferential protonated site strongly correlates to its H-bonded network structures.

Protonated $(methanol)_n-(water)_m$ mixed clusters ($H^+M_nW_m$) are one of fundamental model systems of protonated binary mixed clusters of protic molecules. Many spectroscopic and mass spectrometric studies combined with quantum chemical calculations have been performed on $H^+M_nW_m$ to understand the size dependence of their proton solvation motifs.[39−60] For the small sizes ($n + m \leq \sim 5$), the exhaustive infrared (IR) studies have elucidated the competition between the two ion cores (protonated sites), H_3O^+ and $MeOH_2^+$, with the change of the ratio of the two components.[52,53,55,59,60] The H-bonded network structure changes with the switching of the ion core type. In addition, it has also been demonstrated that the two different dissociation channels (water-loss and methanol-loss) compete with each other and they correlate to the ion core type. The methanol-loss channel is almost exclusive when the H_3O^+ ion core is

Received: April 21, 2017
Revised: July 1, 2017
Published: July 3, 2017

DOI: 10.1021/acs.jpca.7b03762
J. Phys. Chem. A 2017, 121, 5399−5413

formed while the water-loss channel is promoted when the $MeOH_2^+$ ion core is formed.[39,40,42,44,47,58]

In the larger sizes under the water rich condition ($m \geq 5$, and $m \gg n$), IR spectroscopic studies have demonstrated that the H-bonded network structures are basically similar to those of the corresponding neat protonated water clusters, $H^+(H_2O)_{n+m}$.[55−57] This is because methanol preferentially occupies a surface site which is not fully solvated and dangling OH of the water site can be replaced by the methyl group of methanol. A typical example is seen in the well-known magic number cluster of protonated water, $H^+(H_2O)_{21}$.[48,61] It has been demonstrated that the magic number stability is kept to the replacement of at least 8 water molecules by methanol.

On the other hand, under the methanol rich condition ($n \gg m$), mixing of water molecules into the H-bonded network of methanol induces further degree of freedom of H-bond coordination, and this enables to construct more complex network structures than those in neat methanol.[58] The methanol rich binary system has been first discussed in the mass spectrometric studies. Garvey and co-workers have clarified that $H^+M_{8,9}W_1$ are magic number clusters though no magic number behavior is seen in the corresponding sizes of neat H^+M_n.[44] To explain these magic number clusters peculiar to the mixed system, they have proposed that these clusters form water inclusion-structures, in which the H_3O^+ ion core is surrounded by a single ring of methanol. In the viewpoint of the H-bonded network topology, such an H-bonded structure is composed of three H-bonded rings and can be called multiring (MR) structure. Here, we note that PA of water (165 kcal/mol) is smaller than that of methanol (180 kcal/mol).[62] The formation of the MR structure is an evidence of the importance of the solvation energy of the ion core to determine the preferential protonated site. There have also been several collisional or metastable decay channel measurements of $H^+M_nW_1$, and the switch of the preferential dissociation channel with increase of the cluster size has been found.[39,40,43,44,47,48] While the water-loss is the dominant dissociation channel in the $n < 9$ clusters, the methanol-loss becomes dominant at $n \geq 10$. In analogy with the results in the IR photodissociation studies of the small-sized clusters,[58] these results suggest that the switch of the ion core occur from methanol to water at $n = 9−10$. However, the MR structures request the H_3O^+ ion core, and the magic number behavior of $n = 8$ seems to conflict with the ion core switching size suggested by the dissociation measurement studies.[44]

More detailed information on $H^+M_nW_1$ should be obtained by spectroscopy of the clusters combined with theoretical calculations. In 2009, we have reported the IR spectra and quantum chemistry calculations of $H^+M_nW_1$ ($n = 1−9$) to analyze the size dependence of their H-bonded network structures and preferential ion cores.[58] The stable isomer calculations showed that the MR structure is the most stable isomer in $n \geq 6$. The IR spectroscopic signature of the MR structure is the absence of the free OH stretch vibrational band. The observed IR spectra showed a clear trend that the free OH stretch band becomes weaker with increasing size, but the threshold size of the band disappearance could not be definitely determined because of the limit of the quality of the observed spectra. Moreover, direct comparison between the observed spectra and the theoretical calculation results was difficult. This was because of the following problems: (i) The quality of the observed spectra was limited. (ii) While many isomers contribute to the observed spectra, the calculated spectra were based on single isomer structures. (iii) The isomer population should depend on temperature. But the relative stability (Gibbs energies) of the isomers was calculated only at 190 K. On the other hand, temperature of the observed clusters was not clearly determined, and measurements under a different temperature condition were not performed. (iv) The stable isomer search in the calculations was not done systematically but guided only by chemical intuition. Therefore, both the number and the structural diversity of the searched stable structures were limited.

We have also tried to identify the ion core of the clusters in our previous work.[58] In the theoretical calculations, we have estimated that the $MeOH_2^+$ ion core can compete with the H_3O^+ ion core at $n = 3−7$ at 190 K, but the H_3O^+ ion core is dominant in $n \geq 8$ with the appearance of the MR structures. We have found that the preferential IR predissociation channel switches from the water-loss to the methanol-loss at $n = 8−9$. This observation is almost consistent with the theoretical estimation of the ion core type, however, there is still ambiguity of the ion core because of the lack of clear spectroscopic evidence of the H-bonded network structures. Moreover, temperature dependence of the ion core type has not yet been confirmed by the experiment.

In the present study, we revisit the $H^+M_nW_1$ clusters with much improved IR spectroscopic experiments and theoretical simulations. In the experiments, the quality of the observed spectra is remarkably improved, and the threshold size of the MR structures formation is unequivocally determined. Moreover, to examine the temperature effect on the H-bonded network structure and ion core, we observe the spectra of the clusters under the two different conditions. One is warm clusters produced by a supersonic jet expansion. The other is Ar-tagged clusters, in which the upper bound of the internal energy is restricted to hold a weak intermolecular bond to the tag (Ar atom).[2,63−65] The spectra show remarkable changes with the tagging, and this demonstrates the temperature dependence of the H-bonded network structures. In the theoretical simulations, the extensive isomer search is performed by the multiscale modeling approach.[66−68] The temperature dependence on the IR spectra can be directly simulated by computing the contribution of all stable isomers to the partition function based on the harmonic superposition approximation (HSA) method, and the simulated IR spectra are then directly compared with the observed spectra. On the basis of the combination of the experimental spectra and the theoretical simulations, the size and temperature dependence of the H-bonded network structure and ion core is discussed.

II. EXPERIMENTAL METHODS

Size-selective IR spectra of $H^+M_nW_1$ ($n = 6−10$) in the OH stretching vibrational region (2400−3800 cm^{-1}) were measured by IR dissociation spectroscopy using a tandem-type mass spectrometer.[10,65] Part of H-bonded OH stretch bands overlap with CH stretch bands of the methanol moiety in the 2800−3000 cm^{-1} range. Since CH stretch bands are not necessarily informative to determine H-bonded network structures, we used the deuterium-substituted methanol (methanol-$_{d3}$, CD_3OH) sample in this study. The CH stretching vibrations fall to ∼2000 cm^{-1} with the deuteration, and the interference between OH and CH stretch bands is removed in the observed spectra.

The vapor of methanol-$_{d3}$ was seeded (∼0.2%) in the carrier gas of He−Ar (95:5) mixture. Total stagnation pressure was 60

DOI: 10.1021/acs.jpca.7b03762
J. Phys. Chem. A 2017, 121, 5399−5413

atm. The gas was expanded to a vacuum chamber through a high pressure pulsed valve (Even−Lavie valve).[69] Electron ionization by an electron gun (acceleration voltage 200 V) was applied to the supersonic jet expansion. It has been shown that $H^+M_nW_1$ clusters ($n \geq 6$) are generated by ionization of neat methanol clusters.[70] We employed this method to prepare $H^+M_nW_1$ without adding water to the carrier gas. Produced ions were introduced into a mass spectrometer equipped with linearly aligned tandem quadrupole mass filters connected by an octopole ion guide. The cluster size of interest was selected by the first quadrupole mass filter. Then, the size-selected cluster was irradiated by an IR laser within the octopole ion guide and was sent to the second quadrupole mass filter. The second quadrupole mass filter was tuned to pass only the fragment mass produced by vibrational predissociation. An IR spectrum of the size-selected cluster was recorded by monitoring the fragment ion intensity while scanning the IR laser frequency. Both the fragment channels of water-loss and methanol-loss were monitored to measure IR spectra. The IR light was produced by OPO/OPA (LaserVision), and the typical IR power was ∼1 mJ.

To probe the H-bonded network structure and ion-core type under the cold condition, we also prepared the Ar-tagged clusters of $H^+M_nW_1$, and their IR spectra were measured by monitoring the Ar-loss channel. Though we also could observe the (Ar + water)-loss channel in $H^+M_6W_1$, the measured spectrum by monitoring this channel was essentially the same as that obtained by monitoring the Ar-loss channel.

III. COMPUTATIONAL METHODS

The initial input structures of $H^+M_nW_1$ were searched based on an *ab initio* based hierarchical method we have developed over the last 10 years. This method has been applied to the neutral, deprotonated, and protonated water clusters.[66−68,71,72] In the following, we will summarize key steps and the details can be found in the original literatures. The potential energy landscape of these water clusters was explored by using the global searching methods (such as basin-hopping method[73] and genetic algorithms[67] with an accurate empirical OSS2 model[74]). For a given cluster, a database consisting of local minima/intrinsic structures was analyzed and archived based on their hydrogen-bond patterns. From these database, a selected set of intrinsic structures with distinct hydrogen-bonds and structural patterns are then further examined by performing geometric optimization at the B3LYP/6-31+G* level,[46,55,57,58] using the Gaussian09 suite package.[75]

On the basis of the hydrogen-bond patterns of the water clusters, we have examined mixed water and methanol clusters ($H^+M_nW_m$).[56−58] The structure of methanol in these clusters can be generated by replacing the hydrogen atom of free OH in a water molecule by a methyl group (CD_3). This method has been proven to work well for the small-sized clusters ($n + m = 5$ and 6) at all concentrations by Bing et al.[59,60] For larger clusters, both the water-rich[57] and methanol-rich[58] regions have also been explored. In particular, the same methodology has been applied to the protonated methanol clusters of different sizes.[10,25]

In this work, we collected hundreds of $H^+M_nW_1$ isomers (methanol is deuterated ($-d_3$)) using the aforementioned searching and substitution methods. For a given size, intrinsic structures were carefully examined by geometric optimization as well as the frequency calculations using B3LYP/6-31+G* with standard settings (that is fine grid for integration of exchange and correlation functional and tight convergence for geometry optimization) to find the balance between accuracy and the large amount of geometry optimizations. In this work, we obtained 293, 331, and 504 optimized $H^+M_nW_1$ isomers for n = 6, 7, and 8, respectively. To consider a large number of possible isomers that all contribute to the thermal properties of a system, we engaged a quantum harmonic superposition approximation (Q-HSA)[62,76−78] to statistically reconstruct the partition function. To summarize, the total partition function $Z(\beta)$ of an N atom system at temperature T can be expressed as the direct sum of the contributions from all optimized isomers

$$Z(\beta) = \sum_a n_a Z_a(\beta) \tag{1}$$

where the suffix denotes the ath isomer (local minimum) and n_a is the degeneracy factor given by

$$n_a = \frac{2N_C!N_O!N_H!}{m_a} \tag{2}$$

In the case of $H^+M_nW_1$ consisting of three atom types, N_C, N_O, and N_H are number of C, O, and H atoms respectively, and m_a refers to the order of point group symmetry. Under the Q-HSA scheme, each locally optimized isomer is treated as a harmonic and infinite basin which is characterized by its vibrational frequencies and relative energy.[77,78] In the quantum regime, $Z_a(\beta)$ is specified by

$$Z_a^Q(\beta) = \exp(-\beta E_a) \prod_{f=1}^{3N-6} \frac{\exp(-\beta\hbar\omega_f^a/2)}{1 - \exp(-\beta\hbar\omega_f^a)} \tag{3}$$

where $\beta = \left(\frac{1}{k_\beta T}\right)$, k_β is the Boltzmann constant, E_a is the electronic energy, and ω_f^a is the fth vibrational frequency of isomer a multiplied by a scaling factor of 0.973, which was originally introduced by Wang et al. to reproduce the free OH-stretch bands in the experimental spectra of protonated water clusters[79] and it has been applied to various protonated water/methanol clusters.[10,25,57−59,72,80]

As a result, an averaged physical property $Y_{total}(\omega,T)$ at temperature T can be constructed as the weighted sum of $Y_a(\omega)$ with the canonical probability $P_a(T)$ of isomer a where $P_a(T) = Z_a^Q(\beta)/Z(\beta)$. To compute the averaged spectrum, the discrete IR absorption intensity I_f^a of isomer a with respect to the aforementioned scaled harmonic frequency ω_f^a is obtained from the DFT calculations. To convert the stick spectra into the continuous ones, a convolution process with a Lorentzian function is applied to the intensities:

$$I_a(\omega, \Gamma) = \sum_f^{3N-6} \frac{\Gamma}{2\pi\left[(\omega - \omega_f^a)^2 + \left(\frac{\Gamma}{2}\right)^2\right]} I_f^a \tag{4}$$

To simulate the vibrational decay lifetime in the experimental spectra, a power law function of Γ was proposed by Takahashi and co-workers:[81,82]

$$\Gamma = \begin{cases} 20; & \omega_f^a > 3600\ \mathrm{cm}^{-1} \\ \alpha(\Delta\omega)^\beta = \alpha(\omega_{freeOH} - \omega_f^a)^\beta; & \omega_f^a \leq 3600\ \mathrm{cm}^{-1} \end{cases} \tag{5}$$

where $\Delta\omega$ is the red shift of the H-bonded OH band peak with respect to the free OH peak of the experimental spectra. The

DOI: 10.1021/acs.jpca.7b03762
J. Phys. Chem. A 2017, 121, 5399−5413

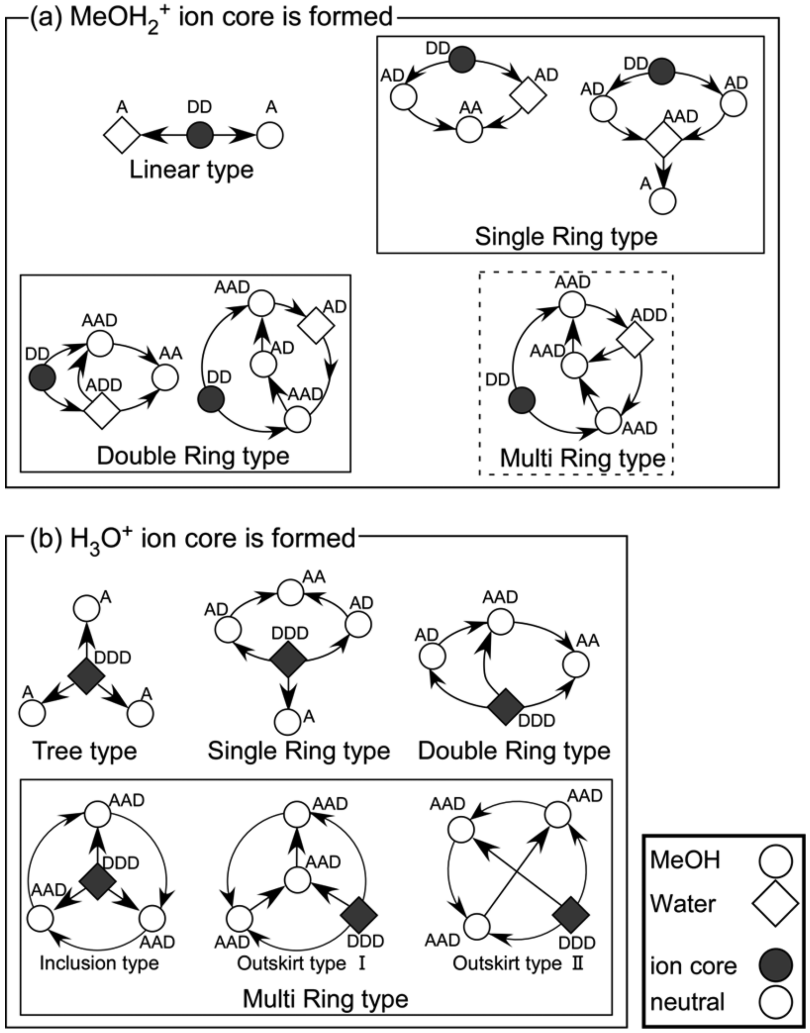

Figure 1. Symbolic representation of hydrogen-bonded (H-bonded) network structures of $H^+(methanol)_n$-$(water)_1$ clusters ($H^+M_nW_1$). (a) Structure types with the methanol ion core ($MeOH_2^+$). (b) Structure types with the water ion core (H_3O^+). Open circle (○) and diamond (◇) represent methanol and water, respectively. Ion cores of methanol and water are represented by closed circle (●) and diamond (◆), respectively. An arrow indicates the direction of H-bond(s) from a proton donor to a proton acceptor. Conformers are neglected in the representation for simplicity. Number of sites (molecules) in each scheme is reduced to clarify the topological feature of each structure type. Note that the Multi-Ring type structure with the methanol ion core is energetically unfavorable (see text).

parameters of Γ, $\alpha = 0.0009$, $\beta = 1.9$, and $\omega_{free\ OH} = 3678\ cm^{-1}$, were previously determined by Hamashima et al. based on fitting to experimental IR spectra of protonated methanol clusters between 3000 to 3600 cm^{-1}.[25]

Finally, the averaged intensity of the whole system can be written as the weighted sum of the spectrum intensity:

$$I_{total}(\omega, \Gamma, T) = \sum_a I_a(\omega, \Gamma) P_a(T) \quad (6)$$

It is worthwhile to mention that after the H-bond topology of the isomers is probed, the partition function as well as the simulated IR spectrum of a specific H-bond network in the isomers such as linear, single ring, double ring, or multiple ring can also be determined.

IV. RESULTS AND DISCUSSION

A. H-Bonded Network Structures. *Categories of H-Bonded Network Structures.* Prior to presentation of the experimental and computational results, we discuss possible H-bonded network structures in $H^+M_nW_1$ on the basis of the H-bond coordination properties of methanol and water. H-bonded network structures are categorized according only to their ion core and network topology in order to simplify the discussion.

H-bonded network structures in $H^+M_nW_1$ can be schematically presented by using the symbols proposed in our previous paper.[23] Representative structures are shown in Figure 1. An open circle (○) represents a methanol molecule and an open diamond (◇) means a water molecule. Closed circle (●) and closed diamond (◆) represent protonated methanol and water site, respectively. An arrow means H-bond(s), and it indicates the direction of the H-bond from a proton donor to a proton acceptor. According to the coordination condition, each site is categorized to A (single-acceptor), D (single-donor), AD (single-acceptor single-donor), AA (double-acceptor), AAD (double-acceptor single-donor), or ADD (single-acceptor double-donor). In the case of an ion core, DD (double-donor) and DDD (triple-donor) sites are also plausible for methanol and water, respectively.

DOI: 10.1021/acs.jpca.7b03762
J. Phys. Chem. A 2017, 121, 5399−5413

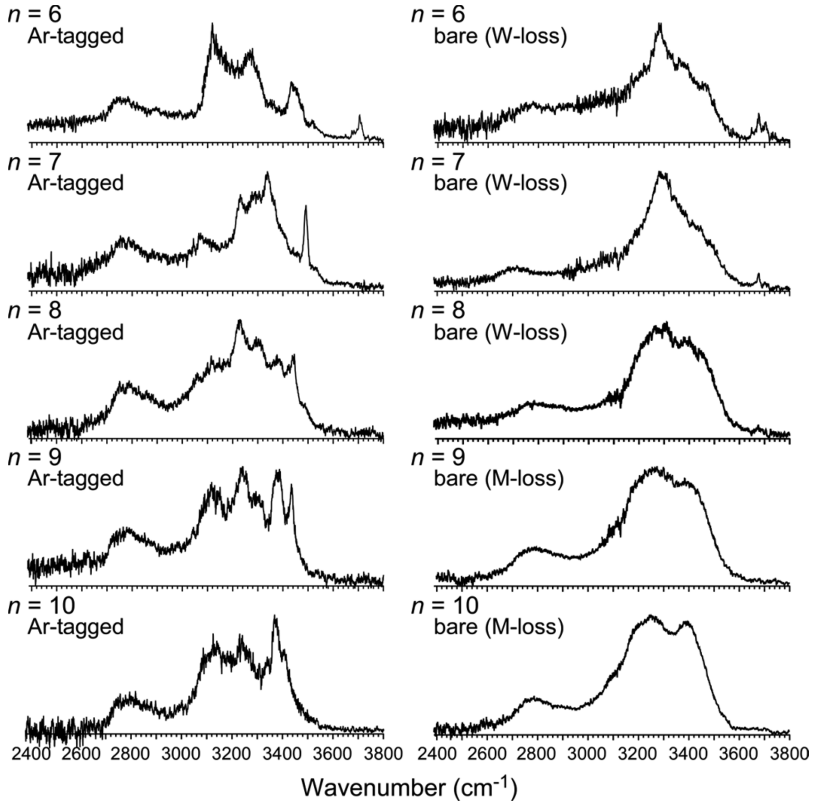

Figure 2. Observed IR spectra of $H^+M_nW_1$ (n = 6−10) in the OH stretch region. The spectra in the left side column are of the Ar-tagged clusters and those in the right side column are of the bare clusters. The major dissociation channel was monitored to measure each spectrum. The monitored channel is indicated in the spectra of the bare cluster.

First, we discuss possible H-bonded network structures with the methanol ion core. H-bonded network structures can be categorized to linear (L), single ring (SR), and double ring (DR) types as shown in Figure 1. In our previous papers, SR and DR are called "cyclic" and "bi-cyclic", respectively, based on the early work on neat methanol clusters.[58] In the present paper, we employ more systematic nomenclatures to treat the mixed system. Various conformations and sequences of molecules are possible for each structure type. In the SR type, an AA site exists in the network, and a side chain terminated by an A site can be formed from this AA site (then, this site becomes an AAD site). Such a structure with a side chain has been called "cyclic with a tail" type. In the present work, however, both the "cyclic" and "cyclic with a tail" types are categorized into the SR type to reduce the number of network types and simplify the display of the HSA calculation results.

The methanol ion core has a strong preference to being the DD coordination. The L type is the simplest structure type with the DD ion core in probable H-bonded network structures. In this type, the ion core extends two H-bond chains, which consist of AD sites and are terminated by A sites. The SR type also has the DD ion core. When the two H-bonded chains from the DD ion core are connected to each other, a single ring consisting of AD sites is formed and the connecting site becomes an AA site. The AA site in the SR type prefers to locate away from the ion core.[58] This is because the two H-bonds to the AA site are weaker than others while the ion core can enhance the strength of neighboring H-bonds. This AA site becomes an AAD site when a side chain extends from the site. This side chain is terminated by an A site. Therefore, it can be bound somewhere in the ring moiety. Then, a DR structure is formed. It has been shown that this structure type is most stable in protonated neat methanol clusters of $n \geq 7$.[10,24,25] We should note that all these isomer types have at least one free OH group in methanol or water sites.

In the case of the water ion core, H_3O^+, the most flexible H-bonded network is tree (T) type structures, since the ion core is preferentially solvated. The water ion core is located at the center and three methanol chains extend from the ion core. When two of these methanol chains are bound to each other, the network changes to the SR type, which is the second most flexible network type with the water ion core. The ion core in SR is also in the DDD coordination. Similar to the SR type of the methanol ion core, the AA site prefers to locate away from the ion core. The SR type with the water ion core still has an H-bond chain from the ion core. The DR structure is formed when this chain is bound to the ring moiety. The DR type is obviously more rigid than the SR type. In this DR type network, there are an AAD site and an AA site of methanol. From the AA site in the DR type, an H-bond chain terminated by an A site can be extended. When this side chain is bound to the ring moiety, the network finally develops to the MR type (this is called "tri-cyclic" structure in our previous paper).[58] MR is the most rigid H-bonded network type in all the conceivable network types of $H^+M_nW_1$. MR has the maximum numbers of three coordinated molecules and hydrogen bonds among all the possible network types. We note that no free OH group exists in MR. There are three subtypes of MR depending on the location of the water ion core. In the inclusion type, the water ion core locates at the center of the H-bonded network, while in the outskirt types I and II, the ion core locates at the

DOI: 10.1021/acs.jpca.7b03762
J. Phys. Chem. A 2017, 121, 5399−5413

periphery of the network. The outskirt types have been found to be more stable in energy than the inclusion type in the previous study.[58] However, the H-bonded network structures could not be definitely determined by the experimental observation because of the limited quality of the spectra and the lack of the theoretical spectra based on the isomer ensemble. In the viewpoint of topology, MR type structures can be formed also with the methanol ion core when the water site becomes an ADD site (see Figure 1a). However, within the observed size range ($n + m \leq \sim 10$), the ADD water site is energetically much unfavorable in comparison with the DDD water ion core. Therefore, population of such a structure is practically excluded.

Observed IR Spectra. The observed IR spectra of $H^+M_nW_1$ (n = 6−10) in the OH stretch region are shown in Figure 2. To compare with temperature dependent theoretical IR spectra (HSA spectra), which reflect the isomer populations, the spectra were measured under the two different conditions. One is the spectra of the Ar-tagged clusters shown in the left side column, and the other is the spectra of the bare clusters displayed in the right side column. Effective temperature of the Ar-tagging cluster is low (typically lower than ca. 100 K), because clusters with internal energy higher than the binding energy with Ar cannot survive due to dissociation. The bare protonated clusters are relatively warmer (typically higher than ca.150 K) because of the large excess energy in the protonation.[10,25,83,84] The observed IR spectra in Figure 2 were measured by monitoring the major dissociation channel of each cluster size. For the bare clusters, the water or methanol-loss channel was monitored, as indicated by W/M-loss in the figure, respectively. The Ar-loss channel was monitored for the Ar-tagged cluster.

Free OH stretch bands are expected in the 3600−3800 cm^{-1} region and H-bonded OH stretch bands appear in the region lower than 3600 cm^{-1}. The two IR spectra of the Ar-tagged and bare clusters at the same size are considerably different from each other. In addition to the wider bandwidth in all the spectra of the bare clusters, difference in the band structure is remarkable especially in n = 6 and 7. This indicates that effective temperature of the clusters falls with the Ar-tagging and the isomer population also largely changes. Moreover, the symmetric and antisymmetric OH stretch (ν_1 and ν_3) bands of an A site water are not observed in the observed spectra. This means that the water molecule in the clusters does not locate at the end of an H-bonded chain network and at least one of the OH groups of the water always acts as a donor.

Isomer Population under the Harmonic Superposition Approximation. Figure 3 shows the temperature dependence of the isomer populations of the n = 6−8 clusters based on the HSA calculations. For each size, the ordinate shows the normalized isomer population ratio and the abscissa shows temperature of the cluster. Each colored line shows a relative population of an isomer structure type. As a general trend, it seems that populations of rigid isomer types, which have more number of hydrogen bonds, are relatively larger in lower temperature, and populations of flexible isomer types, which have less number of hydrogen bonds, become dominant in higher temperature. We should note that in low-temperature many quantum effects (such as anharmonicity, coupling between electron and proton, accuracy of the level of DFT) can be critical, so one should not over interpret the low temperature behavior described by HSA and B3LYP/6-31+G*. Nevertheless, similar temperature dependence of isomer

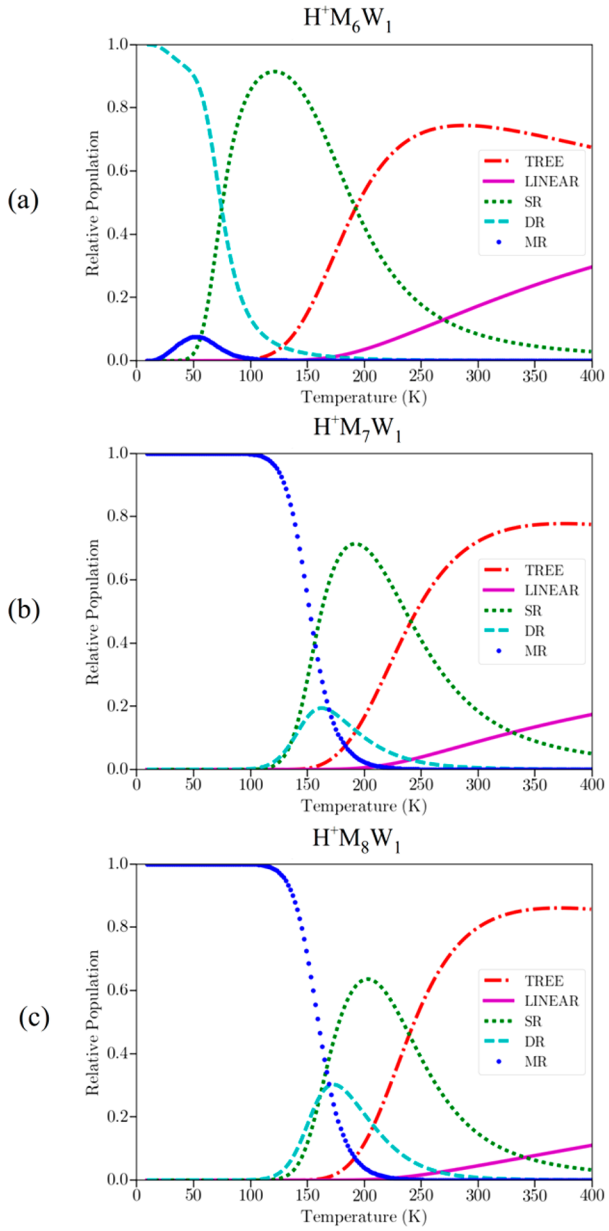

Figure 3. Temperature dependence (3−400 K) of the isomer populations based on the HSA calculations: (a) $H^+M_6W_1$, (b) $H^+M_7W_1$, and (c) $H^+M_8W_1$. The relative populations are normalized. Each colored line shows a population of a structure type. Dotted red, violet, dotted green, broken light blue, and dotted blue lines mean relative population of tree (T), linear (L), single ring (SR), double ring (DR), and multi-ring (MR) structures, respectively.

populations occurs in elevated temperatures has been confirmed for several hydrogen-bonded cluster systems.[10,14,25,26,85−87] Isomer populations are governed by the competition between energy and entropy in free energy. Rigid structures are more stable in energy than flexible structures, being the majority at low temperature. On the other hand, entropy drives populations of flexible structures with rise of temperature because flexible structures have more number of low frequency modes in comparison with rigid structures. The spectral simulations are performed based on these isomer populations. Effective temperature and H-bonded network structures of the observed Ar-tagged and bare clusters are determined by comparison with the theoretical HSA spectra.

DOI: 10.1021/acs.jpca.7b03762
J. Phys. Chem. A 2017, 121, 5399−5413

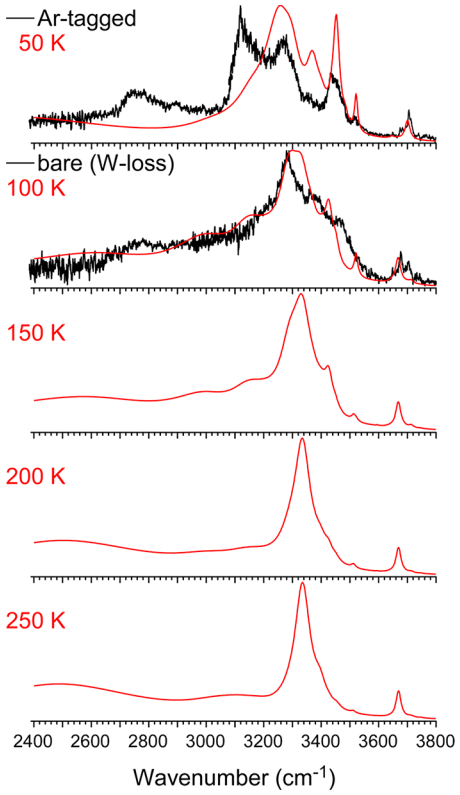

Figure 4. Comparison between the observed IR spectra (black) of bare and Ar-tagged $H^+M_6W_1$ and the HSA spectra (red) calculated at every 50 K in the OH stretch region. Each observed IR spectrum is overlapped with the HSA spectrum which reproduces the observed one best.

n = 6. Figure 4 shows the comparison between the observed IR spectra and the theoretical HSA spectra of $H^+M_6W_1$. The HSA spectra are calculated at every 50 K. Each observed spectrum is overlapped with the HSA spectrum which reproduces the observed one best. The observed spectrum of the Ar-tagged cluster is best reproduced with the HSA spectrum at 50 K, and the HSA spectrum at 100 K simulates well the observed spectrum of the bare cluster. The agreement between the observed and simulated spectra is qualitative. The band at ~3100 cm^{-1} of the spectrum of the Ar tagged cluster is the most prominent disagreement with the simulation. Some of such disagreements may be mainly attributed to the limit in the harmonic oscillator approximation, which results in lack of bands due to coupling with the strong excess proton vibrations. On the whole, however, the large changes of the observed spectral features with and without tagging are reproduced well by the simulations. This means that the calculated isomer population successfully catches the essence of the temperature dependence.

On the basis of the temperature dependence plot of the isomer populations shown in Figure 3a, the Ar-tagged cluster, of which effective temperature is estimated to be ca. 50 K, is dominantly composed of DR type structures. On the other hand, SR type structures are the major component for the bare cluster, which is estimated to be at ca. 100 K. Parts a and b of Figure 5 show examples of DR and of SR structures. We pick up the minimum free energy isomers at 50 and 100 K, respectively. It should be noted that these structures are only a part of the conceivable isomers. Not only the arrangement patterns of methanol and water but also the orientation of the

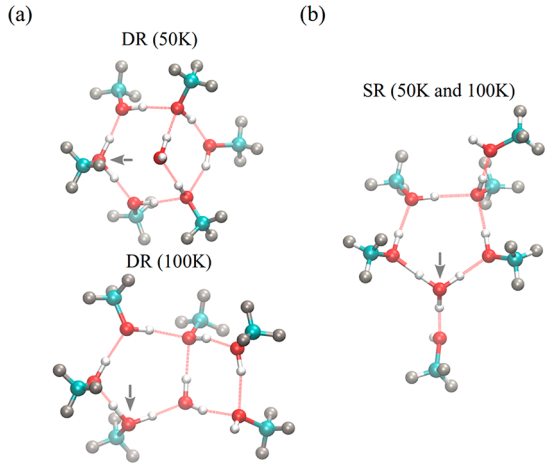

Figure 5. (a) DR and (b) SR structures of $H^+M_6W_1$. The minimum free energy isomer structures at 50 and 100 K are selected among all the searched isomers, respectively. The protonated site is indicated by the arrow.

methyl group produces conformational isomers. A large number of isomers should coexist under the observed conditions.

On the basis of the above-mentioned comparison with the HSA spectra, the effective temperature of the bare cluster is estimated to be ca. 100 K. This value is lower than that (150−200 K) of the other protonated clusters (e.g., $H^+(CH_3OH)_n$) produced by the same type of the ion source in our previous studies.[10] As will be shown later, the observed spectral features weakly depend on the monitoring dissociation channel (water-loss or methanol-loss). This is due to the correlation among the H-bonded structure, ion core type, and preferential dissociation channel. Therefore, the observed spectra may not necessarily reflect the exact isomer distribution, and contribution of some specific isomer types can be suppressed (or enhanced). At the 150−200 K region, the T type structures, which exclusively have the water ion core, strongly compete with the SR type structures. Since the observed spectrum of the bare cluster of *n* = 6 shown in Figures 2 and 4 was measured by monitoring the water-loss channel (major dissociation channel), the contribution of the T type structures to the spectrum can be largely suppressed if the methanol-loss is the major dissociation channel of the T type structures. In this case, the observed IR spectrum seemingly reflects the population at 100 K in which population of the T type structures is much suppressed. Determination of the accurate temperature of the bare cluster is difficult in the present experiment. However, from the remarkable changes of the spectrum with the tagging, it is certain that the large isomer population changes occurs between the Ar-tagged and bare clusters (different temperature ranges).

n = 7. Also in *n* = 7, the HSA calculations predict strong temperature dependence of the isomer population (see Figure 3b). The MR structures become the most stable isomer type in *n* = 7 and they are dominant in the low temperature range. Figure 6 shows the comparison between the observed and HSA spectra of the *n* = 7 cluster. The observed spectrum of the Ar-tagged cluster is best reproduced by the simulation at 50 K, while that of the bare cluster is by the simulation at 150 K. The agreement between the simulation at 50 K and the observed spectrum of the Ar-tagged cluster seems better than that in *n* = 6. Moreover, we should note that no free OH stretch band is

DOI: 10.1021/acs.jpca.7b03762
J. Phys. Chem. A 2017, 121, 5399−5413

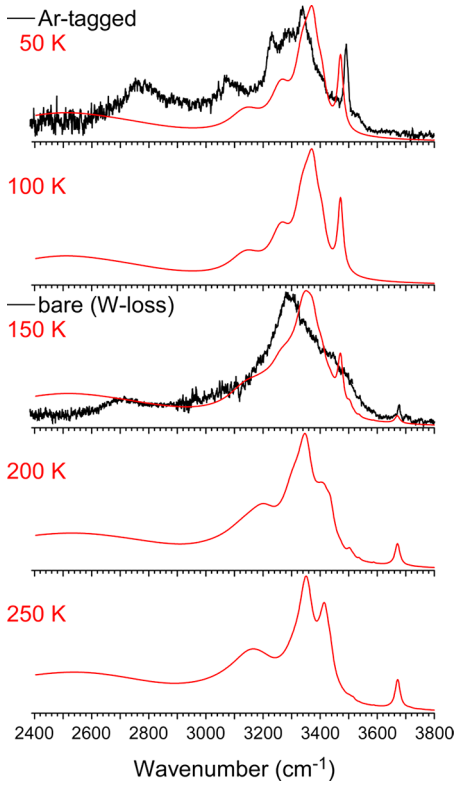

Figure 6. Comparison between the observed IR spectra (black) of bare and Ar-tagged $H^+M_7W_1$ and the HSA spectra (red) calculated at every 50 K in the OH stretch region. Each observed IR spectrum is overlapped with the HSA spectrum which reproduces the observed one best.

seen in the observed spectrum of the Ar-tagged cluster. This means that all the OH groups in the cluster form H-bonds. This characteristic occurs only in the MR structures, which are predicted to be dominant in the cold condition (Figure 3b). Therefore, the lack of the free OH band in the observed spectrum is definite evidence for the dominance of the MR structures. The MR structure of the lowest free energy at 50 K is shown in Figure 7a. We note that the outskirt type II of the MR structures is the most stable isomer. There are also low-lying similar type isomers, and the observed spectrum should involve contribution of them.

On the other hand, a free OH stretch vibration band of methanol is observed in the spectrum of the bare cluster, which is best simulated at 150 K. The isomer population calculation in

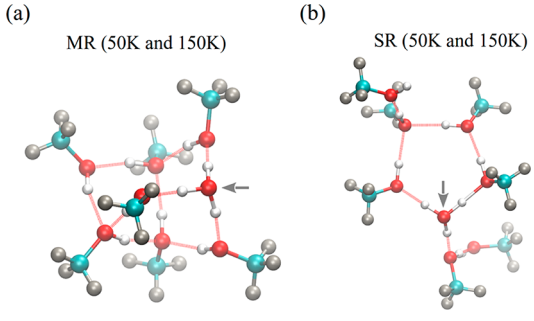

Figure 7. (a) MR structure of $H^+M_7W_1$ of the minimum free energy at 50 and 150 K. (b) SR structure of the minimum free energy at 50 and 150 K.

Figure 3b shows that SR structures strongly compete with MR structures at 150 K. SR structures should have a dangling OH, and the contribution of SR structures is consistent with the observed spectrum. Because SR structures are more flexible than MR structures, entropy drives the population of the SR structures with elevation of temperature. Figure 7b shows the SR structure which has the lowest Gibbs energy at 150 K. Also note that this is one of the many isomers contributing to the observed spectrum.

n = 8. Figure 3c displays the calculated temperature dependence of the isomer population of $n = 8$. The isomer population behavior seems very similar to that of $n = 7$. It also shows a clear trend that rigid MR structures with more H-bonds are preferential in low temperature and more flexible structures with a less number of H-bonds become major isomers in high temperature. The MR structures are dominant up to 150 K.

Figure 8 shows the comparison between the observed and HSA spectra. The spectrum of the Ar-tagged cluster is

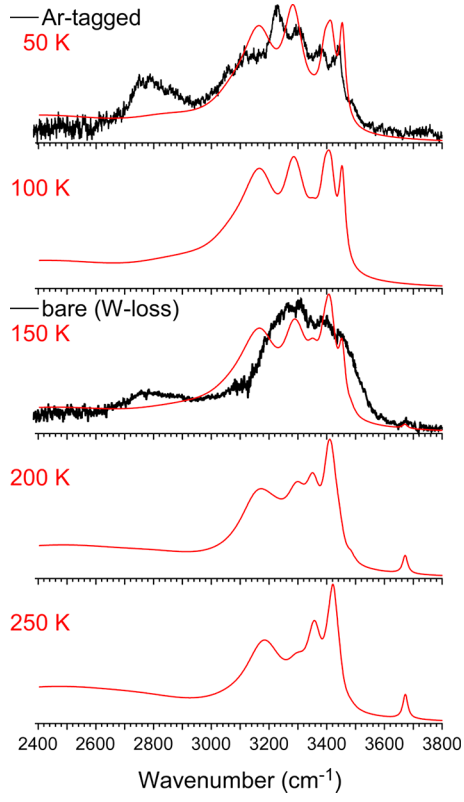

Figure 8. Comparison between the observed IR spectra (black) of bare and Ar-tagged $H^+M_8W_1$ and the HSA spectra (red) calculated at every 50 K in the OH stretch region. Each observed IR spectrum is overlapped with the HSA spectrum which reproduces the observed one best.

reproduced best by the simulation at 50 K also in this size. Missing of the free OH stretch band strongly supports the dominant population of the MR structures, being consistent with the temperature dependence calculation. The MR structure of the lowest free energy at 50 K is shown in Figure 9a. Also in this size, the most stable MR structure is of the outskirt type II.

In the observed spectrum of the bare cluster, a very weak band of free OH stretch vibration is still seen. This indicates

DOI: 10.1021/acs.jpca.7b03762
J. Phys. Chem. A 2017, 121, 5399−5413

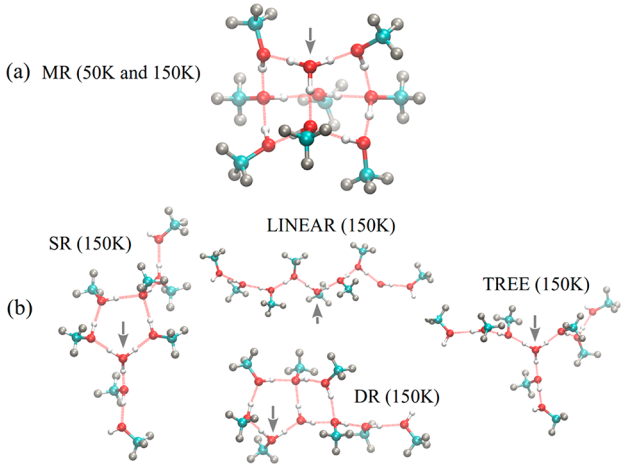

Figure 9. (a) MR structure of $H^+M_8W_1$ of the minimum free energy at 50 and 150 K. (b) Structures of the minimum free energy at 150 K in each isomer type.

small contribution of isomers other than the MR structures. The HSA spectrum at 150 K reproduces best the observed spectrum though the agreement is qualitative. SR and DR structures are expected to coexist with MR structures at 150 K, and they contribute to the weak free OH stretch band. As an example of the possible spectral carrier, the structure which has the lowest free energy at 150 K in each isomer type is shown in Figure 9b. The reproducibility of the observed spectrum by the simulation may be restricted by some reasons. At high temperature, broadening of the band seems to be remarkable. Though presence of hot bands would be its main origin, inclusion of its effect is very difficult in the present approach since such a simulation requests anharmonic calculations.

n = 9–10. Since there are too many possible structures and the DFT calculations become too expensive, HSA spectra were not calculated in this size region. However, the observed structure type can be determined without theoretical calculations because the free OH band clearly disappears in both the spectra of the bare and Ar-tagged clusters, as shown in Figure 2. This clearly indicates that MR structures are predominant in this size region at the wide range of temperature.

As described in the previous section, there are three types for MR structures; inclusion type (the water ion core locates at the center of the methanol ring) and outskirt types I and II (the water ion core locates within the outer ring). Though the theoretical calculations predict that the outskirt types are more stable in energy than the inclusion type, it is difficult to determine the type of the MR structure from the observed spectra in the H-bonded OH stretch region. Marker bands to distinguish these two structure types are expected in below 2400 cm^{-1}, which is out of the present measurement frequency range. Observation of these bands is future task to identify the most stable type of the MR structures.

B. Ion Core (Protonated Site) Determination. Determination of the preferential ion core is also an important subject in the protonated mixed cluster study because the ion core plays a central role in proton transfer and is closely related to H-bonded network structures. In our previous study, the preferential ion core of $H^+M_nW_1$ was probed by the IR spectroscopy, dissociation fragment channel measurements, and theoretical calculations.[58] However, the quality of the observed IR spectra was limited, and the preferential ion core was essentially inferred only from the major dissociation channel. The theoretical analysis was also difficult because too many isomers are possible for hand construction of the initial structures and the temperature dependence was not seriously examined. Therefore, in the present up-dated experimental and theoretical approaches, we examine the preferential ion core and its size and temperature dependence both from IR spectroscopy and HSA simulations.

The ion core can be experimentally determined by analyzing the free OH stretch region of the measured IR spectra. Since

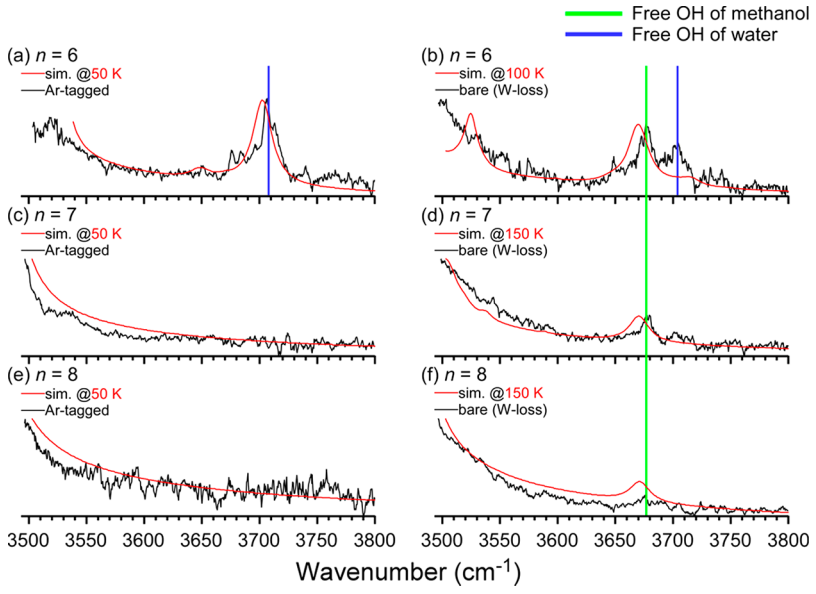

Figure 10. Expanded free OH stretch region of the observed IR spectra (black curves) and HSA spectra (red curves) of $H^+M_nW_1$ (n = 6–8). Temperature of each HSA spectrum is selected by the best fit in the whole OH stretch region. The IR spectra in the left side column (a, c, e) are those of the Ar-tagged clusters and the right column (b, d, f) shows those of the bare clusters. The green and blue markers indicate the frequencies of the free OH bands of methanol (3680 cm^{-1}) and 2- or 3-coordinated (AD or AAD) water (3700 cm^{-1}), respectively.

DOI: 10.1021/acs.jpca.7b03762
J. Phys. Chem. A 2017, 121, 5399–5413

the excess charge enhances the electrostatic interaction and induction, the H-bonds of the ion core are the strongest ones in the cluster. Therefore, the ion core is preferentially solvated, and no free OH of the ion core should appear in IR spectra in the observed size region. Furthermore, a free OH band of the water moiety can be distinguished from that of the methanol moiety because the frequency of water dangling OH (~3700 cm^{-1}) is different from that of methanol (~3680 cm^{-1}).[1,3,5,10,22,25] If the protonated site is water (H_3O^+), the free OH stretch band of water is not observed because $H^+M_nW_1$ has only one water molecule. On the other hand, if the protonated site is methanol ($MeOH_2^+$), only the free OH stretch band of water or those both of water and methanol are observed. Size and temperature dependence of the protonated site is also estimated by the population weight of the isomers in the HSA calculation.

Figure 10 shows the expanded free OH stretch region of the observed spectra of $H^+M_{6-8}W_1$ (black curves). The red curves in the figure are the HSA spectra at the temperature determined by the comparison with the observed spectra of the whole OH stretch region in the previous section. Note that the free OH band totally disappears in the spectra both of the bare and Ar-tagged clusters of n = 9 and 10 though their expanded spectra are omitted in Figure 10.

In Figure 10, the spectra in the left side column are those under the cold condition (ca. 50 K, Ar-tagged clusters) and the spectra in the right column are under the warm condition (100−150 K, bare clusters). The green and blue markers indicate the frequencies of the free OH bands of methanol (3680 cm^{-1}) and 2- or 3-coordinated water (3700 cm^{-1}), respectively. The two free OH bands characteristic of 1-coordinated (single acceptor) water, ν_1 and ν_3, are not observed in all the observed sizes ($6 \leq n \leq 10$).

n = 6. Parts a and b of Figure 10 show the IR spectra of $H^+M_6W_1$ of the Ar-tagged and bare clusters, respectively. The relative intensity of the methanol and water free OH stretch bands significantly changes with the Ar tagging. With the Ar-tagging, the water free OH band is almost exclusively seen in the spectrum, while the methanol free OH band is superior to the water free OH band in the bare cluster. This spectral change should correlate with the change of the ion core as well as the H-bonded network structures.

The preferential ion core is determined by the observed IR spectra. The exclusive appearance of the water free OH band under the cold condition indicates that the excess proton is preferentially accommodated by methanol. Figure 11a shows the population ratio of the ion core provided by the HSA calculations. At 50 K, the dominant population of the methanol ion core is predicted, and this agrees well with the observation. The dominance of the methanol ion core at the low temperature range correlates with the preference of the DR structures, as seen in the temperature dependence of the isomer types (see Figure 3a).

On the other hand, under the warm condition, the free OH bands of both water and methanol are seen in the observed spectrum. This suggests that the methanol ion core and water ion core coexist. The HSA simulation predicts the coexistence of the two ion cores in temperature higher than ca. 50 K, and the water ion core is superior to the methanol ion core in temperature higher than 75 K (see Figure 11a). The increase of the water ion core comes from the contribution of the SR and T structures (see Figure 3a). This theoretical prediction is consistent with the observation. The HSA spectrum at 100 K,

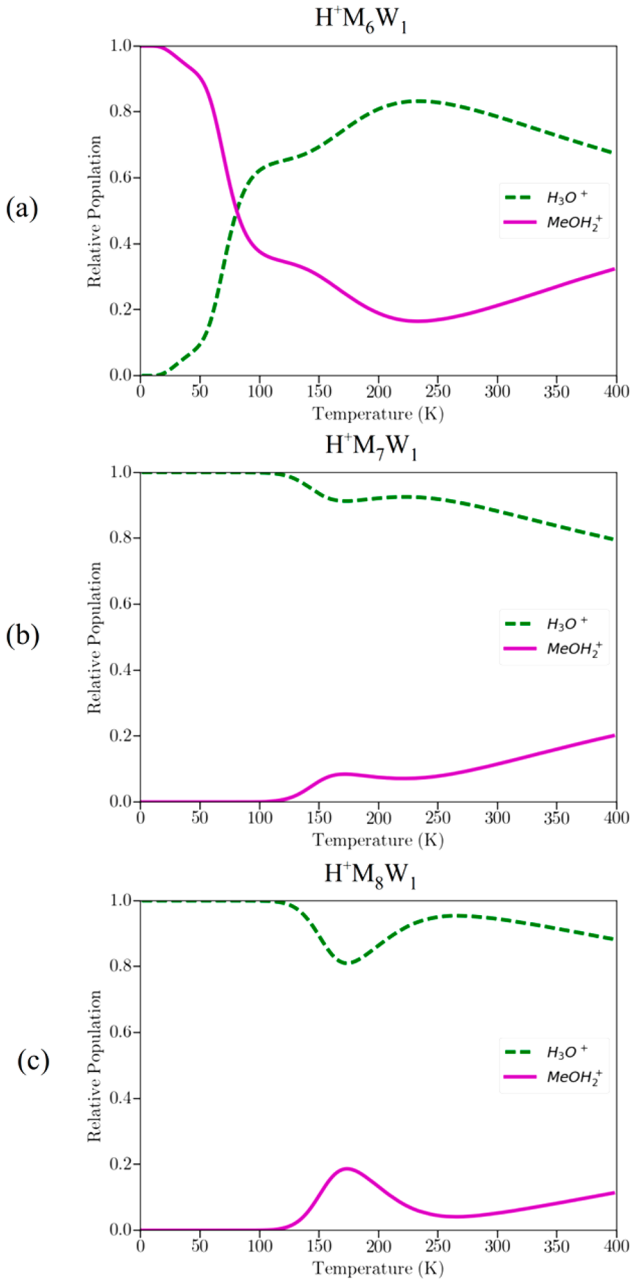

Figure 11. Relative population ratio of the ion cores provided by the HSA calculations at each size ((a) $H^+M_6W_1$, (b) $H^+M_7W_1$, and (c) $H^+M_8W_1$). The temperature dependence starts from 3 to 400 K. The purple and the dotted green curves show the populations of the methanol ($MeOH_2^+$) and water (H_3O^+) ion cores, respectively.

which reproduces best the overall observed spectrum in the full OH stretch region, somewhat underestimates the intensity of the water free OH band in the observed spectrum. This may be attributed to the bias due to the monitored fragment channel, as partly discussed in section IV.A. This spectrum was measured by monitoring the water-loss channel, and the contribution of the water ion core isomers (having methanol free OH) tends to be suppressed (another sign of such intensity bias is discussed in section IV.C). This enhances the relative intensity of the water free OH band. There may be also the contribution of the uncertainty in the effective temperature, which is sampled only at every 50 K for the spectral simulation

DOI: 10.1021/acs.jpca.7b03762
J. Phys. Chem. A 2017, 121, 5399−5413

though the relative population of the two ion cores steeply changes in the temperature range between 50 and 150 K.

n = 7–10. In this size region, any free OH stretch band is not observed under the cold condition (with the Ar-tagging), and the HSA spectra reproduce well the observed spectra, as shown in parts c and e of Figure 10. This indicates that all the OH groups in the clusters form H-bonds, and only the MR structures satisfy this condition. In the MR structures, the ion core is uniquely water. Under the warm condition, a very weak free OH band of the methanol moiety is observed in n = 7 and 8 (Figure 10, parts d and f), and this demonstrates the minor population of structures other than the MR structures.

In order to determine the ion core, these results of the observed spectra are compared with the HSA calculations. Parts b and c of Figure 11 show the calculated population ratio of the two ion cores at n = 7 and 8, respectively. The water ion core is dominant irrespective of temperature in both sizes. In particular, at the low temperature range (<ca. 100 K), the exclusive population of the MR structures results in the dominance of the water ion core. For the minor population of the methanol ion core, the hump seen at around 150 K is attributed to the population of the DR structures, and the gradual rise at temperature higher than 200–250 K correlates to the most flexible linear type structures. The HSA simulations of the ion core agree well with the observed temperature dependence of the spectral behavior.

As was described above, any free OH band is not observed in n = 9 and 10 irrespective of temperature. Though HSA calculations were not performed in these sizes, the absence of the free OH stretch band uniquely indicates the predominance of the MR structures which have the water ion core.

On the preferential ion core, as a whole, the ion core switching (change of the ion core with temperature) is observed at n = 6 and the clear preference of the water ion core is seen in the larger size. These findings demonstrate that the preferential ion core is not simply determined by the magnitude of the proton affinity of the protonated molecule but it strongly depends on the free energy of the H-bonded structures of the cluster, which strongly correlate to the ion core type. While the water ion core (H_3O^+) can be a triple donor site, the methanol ion core ($MeOH_2^+$) can be a double donor at most. Therefore, more number of solvent molecules can directly interact with the ion core if water is the protonated molecule (ion core). This may be the background of the preference of the water ion core in the larger sized clusters, in which the number of molecules involved is enough to surround the ion core.

C. Correlation between the Ion Core and Preferential Dissociation Channel. The IR spectra of the bare clusters shown in Figure 2 were measured by detecting the major dissociation channel. The major channel is the water-loss in the clusters of $n < 9$, and it switches to the methanol-loss in $n \geq 9$, as shown in Table 1. This trend is same as that observed in our previous study,[58] and also is consistent with the collision induced dissociation reported by Stace and co-workers.[39,40] Since the ion core is most strongly solvated by the neighboring neutral molecules, it seems reasonable to assume that dissociation (evaporation) of the ion core hardly occurs. In the (warm) bare clusters of n = 6–8, however, the preferential dissociation of the water molecule was observed though the water molecule is the dominant ion core in these sizes. This indicates that large rearrangement of the cluster structure including proton migration occurs prior to dissociation of the cluster due to IR excitation, and the preferential dissociation channel does not necessarily reflect the preferential ion core. In the present study, we unequivocally determined the ion core type in the clusters based on the spectral features and theoretical simulations. Therefore, the proton migration prior to dissociation is definitely concluded.

Table 1. Relative Yields of the Dissociation Channels of the Bare $H^+M_nW_1$ Clusters Following the Vibrational Excitation at 3240 cm^{-1}

size (n)	water loss	methanol loss
6	0.7	0.3
7	0.8	0.2
8	0.7	0.3
9	0.2	0.8
10	0.0[a]	1.0

[a]The relative yield is not definitely zero and the IR spectrum is measurable by monitoring a trace of the water-loss channel fragment.

While the proton migration definitely occurs in dissociation of the bare clusters, we also found some evidence for the weak correlation between the ion core and preferential dissociation channel, which indicates that the proton migration still competes with dissociation at least in the smaller sizes. Two IR spectra of the bare clusters can be measured by monitoring the two (water-loss and methanol-loss) dissociation channels. The observed spectral features actually somewhat change depending on the monitored channel in the sizes of n = 6–8 (see Figure S1 in the Supporting Information). In n = 6, the monitored channel dependence of the spectra is especially remarkable. Therefore, its characteristics are examined in this section.

Figure 12 shows the IR spectra of $H^+M_6W_1$ measured by monitoring (a) the major water-loss channel and (b) the minor methanol-loss channel. Spectrum a is a reproduction of those in Figures 2 and 4. The band structure around 3400 cm^{-1} is clearly different between these two IR spectra; while spectrum a shows a clear shoulder band but this shoulder disappears in spectrum b. This shoulder band at 3400 cm^{-1} is a marker band of the ring motif in the H-bonded networks of protonated methanol,[10,24] and it is attributed to the H-bonded OH group, which donates the proton to the double-acceptor site in the ring. The strength of this H-bond is especially weaker than

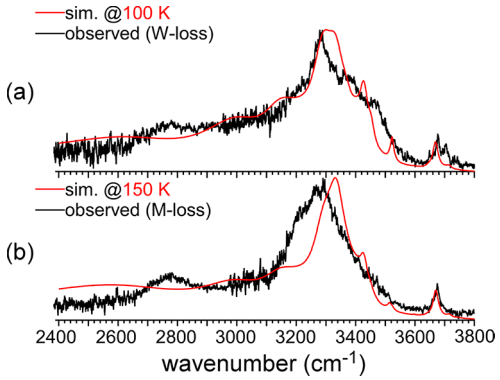

Figure 12. Observed IR spectra (black curves) of $H^+M_6W_1$ by monitoring (a) the water-loss (major) dissociation channel and (b) the methanol-loss (minor) dissociation channel. HSA spectra (red curves) at the best fit temperature are overlapped to the observed spectra. Spectrum a is reproduced from Figure 2.

DOI: 10.1021/acs.jpca.7b03762
J. Phys. Chem. A 2017, 121, 5399–5413

others and the frequency is highest among the H-bonded OH stretches. Moreover, both the (methanol and water) free OH bands appear in spectrum a, but the water free OH band is missing in spectrum b. As discussed in section IV.A, the observed features in spectrum a are reproduced best by the HSA simulation at 100 K, and are interpreted by the major contribution of the SR type structures with the methanol ion core. On the other hand, the features of spectrum b are consistent with the T type structures, which have the water ion core and no double acceptor site in the H-bond networks. The HSA calculation of n = 6 (Figure 3b) shows that the T type structures largely populate in the higher temperature region (ca. 150 K). The HSA spectrum at 150 K reproduces spectrum b better than that at 100 K though the agreement is rather qualitative. This indicates that the monitor of the minor methanol-loss channel preferentially detects the contribution of the T structures of the water ion core.

This result suggests that in binary component clusters, in which multiple dissociation channels compete with each other, fragment-detected IR predissociation spectra can be influenced by the preference of the dissociation channel correlated with H-bonded network structures.[46,88] In the present case, however, as seen in Table 1, the relative weight of the minor channel is lower than ∼30% in each size, and the discussion based on the major channel detection is not seriously affected by the presence of the minor channel. Moreover, the IR spectra of n = 9 and 10 do not show the monitored channel dependence. This suggests that the proton migration competes with the rearrangement of H-bonded networks prior to the dissociation, and the correlation between the ion core and the preferential dissociation channel is washed out in these clusters.

V. CONCLUSION

The H-bonded network structures of the $H^+M_nW_1$ (n = 6−10) clusters were revisited by the combined experimental and theoretical approaches. The IR spectra of the clusters in the OH stretch region were observed at the two different temperature ranges. A few hundreds of stable isomer structures of the clusters of a given size were theoretically searched by the multiscale modeling approach and temperature dependence of the isomer populations and IR spectra were calculated by the HSA method. The observed spectra were qualitatively reproduced by the HSA spectra which include the information on the cluster temperature and the relative population among the isomers. The isomer distribution of the clusters was determined by the comparison between the observed and simulated spectra. At n = 6, remarkable temperature dependence of the dominant isomer type was found and it was interpreted by the entropy term. The formation of the characteristic MR structures was confirmed both by the observed IR spectra and the HSA simulations. At n = 7, the MR structures are formed only at the low temperature range. At n > 8, however, the MR structures are dominant in the range of temperature we observed in this study.

The preferential ion core type was also determined by the observation of the free OH stretch band region and the results were consistent with the HSA simulations. The threshold size for the switch of the ion core from methanol to water depends on temperature. At n = 6, while the ion core is exclusively methanol at low temperature, the major ion core changes to water at high temperature. At n > 7, the preferential ion core is water irrespective of temperature. The major dissociation channel upon the vibrational excitation was same as that in the previous several reports, however, it conflicts with the naive prediction of the preferential dissociation channel based on the ion core type of the cluster. This indicates the migration of the excess proton prior to the dissociation. The weak monitoring channel dependence of the observed IR spectra was also found at n = 6−8. This suggests that the proton migration competes with the dissociation in these sizes.

■ ASSOCIATED CONTENT

Supporting Information

These materials are available free of charge via the Internet at The Supporting Information is available free of charge on the ACS Publications website at DOI: 10.1021/acs.jpca.7b03762.

Comparison between IR spectra obtained by monitoring different dissociation channels and complete author list of ref 75 (PDF)

■ AUTHOR INFORMATION

Corresponding Authors

*E-mail: asukafujii@m.tohoku.ac.jp (A.F.).
*E-mail: jlkuo@pub.iams.sinica.edu.tw (J.-L.K.).

ORCID

Asuka Fujii: 0000-0002-6854-9636

Author Contributions

‡M.K. and P.-J.H. contributed equally to this study.

Notes

The authors declare no competing financial interest.

■ ACKNOWLEDGMENTS

We would like to acknowledge Dr. Toshihiko Maeyama and Dr. Yoshiyuki Matsuda for their helpful discussions. This study was partly supported by a Grant-in-Aid for Scientific Research (Project No. 26288002) from JSPS, Academia Sinica (101-CDA-M06) and the Ministry of Science and Technology (MOST) (MOST 105-2119-M-001-040-MY3 and MOST 105-2113-M-001-006). P.-J.H. and J.-L.K. express thanks for the computing resources provided by Academia Sinica and National Center for High-Performance Computing.

■ REFERENCES

(1) Jiang, J. C.; Wang, Y. S.; Chang, H. C.; Lin, S. H.; Lee, Y. T.; Niedner-Schatteburg, G.; Chang, H. C. Infrared Spectra of $H^+(H_2O)_{5-8}$ Clusters: Evidence for Symmetric Proton Hydration. *J. Am. Chem. Soc.* **2000**, *122*, 1398−1410.

(2) Douberly, G. E.; Walters, R. S.; Cui, J.; Jordan, K.; Duncan, M. A. Infrared Spectroscopy of Small Protonated Water Clusters, $H^+(H_2O)_n$ (n = 2−5): Isomers, Argon Tagging, and Deuteration. *J. Phys. Chem. A* **2010**, *114*, 4570−4579.

(3) Heine, N.; Fagiani, M. R.; Rossi, M.; Wende, T.; Berden, G.; Blum, V.; Asmis, K. R. Isomer-Selective Detection of Hydrogen-Bond Vibrations in the Protonated Water Hexamer. *J. Am. Chem. Soc.* **2013**, *135*, 8266−8273.

(4) Fournier, J. A.; Wolke, C. T.; Johnson, M. A.; Odbadrakh, T. T.; Jordan, K. D.; Kathmann, S. M.; Xantheas, S. S. Snapshots of Proton Accommodation at a Microscopic Water Surface: Understanding the Vibrational Spectral Signatures of the Charge Defect in Cryogenically Cooled $H^+(H_2O)_{n=2-28}$ Clusters. *J. Phys. Chem. A* **2015**, *119*, 9425−9440.

(5) Fujii, A.; Mizuse, K. Infrared Spectroscopic Studies on Hydrogen-Bonded Water Networks in Gas Phase Clusters. *Int. Rev. Phys. Chem.* **2013**, *32*, 266−307.

DOI: 10.1021/acs.jpca.7b03762
J. Phys. Chem. A 2017, 121, 5399−5413

(6) Fridgen, T. D.; McMahon, T. B.; MacAleese, L.; Lemaire, J.; Maitre, P. Infrared Spectrum of the Protonated Water Dimer in the Gas Phase. *J. Phys. Chem. A* **2004**, *108*, 9008−9010.
(7) Fridgen, T. D.; MacAleese, L.; McMahon, T. B.; Lemaire, J.; Maitre, P. Gas Phase Infrared Multiple-Photon Dissociation Spectra of Methanol, Ethanol and Propanol Proton-Bound Dimers, Protonated Propanol and the Propanol/Water Proton-Bound Dimer. *Phys. Chem. Chem. Phys.* **2006**, *8*, 955−966.
(8) Tono, K.; Kuo, J.-L.; Tada, M.; Fukazawa, K.; Fukushima, N.; Kasai, C.; Tsukiyama, K. Infrared Photodissociation Spectroscopy and Density-Functional Calculations of Protonated Methanol Cluster Ions: Solvation Structures of an Excess Proton. *J. Chem. Phys.* **2008**, *129*, 084304.
(9) Solcà, N.; Dopfer, O. IR Spectrum and Structure of Protonated Ethanol Dimer: Implications for the Mobility of Excess Protons in Solution. *J. Am. Chem. Soc.* **2004**, *126*, 9520−9521.
(10) Li, Y. − C.; Hamashima, T.; Yamazaki, R.; Kobayashi, T.; Suzuki, Y.; Mizuse, K.; Fujii, A.; Kuo, J. − L. Hydrogen-Bonded Ring Closing and Opening of Protonated Methanol Clusters $H^+(CH_3OH)_n$ (n = 4−8) with the Inert Gas Tagging. *Phys. Chem. Chem. Phys.* **2015**, *17*, 22042−22053.
(11) Price, J. M.; Crofton, M. W.; Lee, Y. T. Vibrational Spectroscopy of the Ammonlated Ammonlum Ions $NH_4^+(NH_3)_n$ (n = 1−10). *J. Phys. Chem.* **1991**, *95*, 2182−2195.
(12) Yang, Y.; Kühn, O.; Santambrogio, G.; Goebbert, D. J.; Asmis, K. R. Vibrational Signatures of Hydrogen Bonding in the Protonated Ammonia Clusters $NH_4^+(NH_3)_{1-4}$. *J. Chem. Phys.* **2008**, *129*, 224302.
(13) Katada, M.; Shishido, R.; Fujii, A. Infrared Spectroscopy of Large-Sized Neutral and Protonated Ammonia Clusters. *Phys. Chem. Chem. Phys.* **2014**, *16*, 7595−7601.
(14) Malloum, A.; Fifen, J. J.; Dhaouadi, Z.; Nana Engo, S. G.; Jaidane, N.-E. Structures and Spectroscopy of Protonated Ammonia Clusters at Different Temperatures. *Phys. Chem. Chem. Phys.* **2016**, *18*, 26827−26843.
(15) Stoyanov, E. S.; Stoyanova, F. V.; Reed, C. A. IR Spectroscopic Properties of $H(MeOH)_n^+$ Clusters in the Liquid Phase: Evidence for a Proton Wire. *Chem. - Eur. J.* **2008**, *14*, 3596−3604.
(16) Silverman, D. N.; McKenna, R. Solvent-Mediated Proton Transfer in Catalysis by Carbonic Anhydrase. *Acc. Chem. Res.* **2007**, *40*, 669−675.
(17) Hoerner, J. K.; Xiao, H.; Dobo, A.; Kaltashov, I. A. Is There Hydrogen Scrambling in the Gas Phase? Energetic and Structural Determinants of Proton Mobility within Protein Ions. *J. Am. Chem. Soc.* **2004**, *126*, 7709−7717.
(18) Marx, D.; Tuckerman, M. E.; Hutter, J.; Parrinello, M. The Nature of the Hydrated Excess Proton in Water. *Nature* **1999**, *397*, 601−604.
(19) Miyazaki, M.; Fujii, A.; Ebata, T.; Mikami, N. Infrared Spectroscopic Evidence for Protonated Water Clusters Forming Nanoscale Cages. *Science* **2004**, *304*, 1134−1137.
(20) Shin, J. − W.; Hammer, N. I.; Diken, E. G.; Johnson, M. A.; Walters, R. S.; Jaeger, T. D.; Duncan, M. A.; Christie, R. A.; Jordan, K. D. Infrared Signature of Structures Associated with the $H^+(H_2O)_n$ (n = 6 to 27) Clusters. *Science* **2004**, *304*, 1137−1140.
(21) Heine, N.; Fagiani, M. R.; Asmis, K. R. J. Disentangling the Contribution of Multiple Isomers to the Infrared Spectrum of the Protonated Water Heptamer. *J. Phys. Chem. Lett.* **2015**, *6*, 2298−2304.
(22) Chang, H. − C.; Jiang, J. − C.; Lin, S. H.; Lee, Y. T.; Chang, H. − C. Isomeric Transitions between Linear and Cyclic $H^+(CH_3OH)_{4,5}$: Implications for Proton Migration in Liquid Methanol. *J. Phys. Chem. A* **1999**, *103*, 2941−2944.
(23) Fujii, A.; Enomoto, S.; Miyazaki, M.; Mikami, N. Morphology of Protonated Methanol Clusters: An Infrared Spectroscopic Study of Hydrogen Bond Networks of $H^+(CH_3OH)_n$ (n = 4−15). *J. Phys. Chem. A* **2005**, *109*, 138−141.
(24) Kuo, J. − L.; Fujii, A.; Mikami, N. Theoretical Analyses of the Morphological Development of the Hydrogen Bond Network in Protonated Methanol Clusters. *J. Phys. Chem. A* **2007**, *111*, 9438−9445.
(25) Hamashima, T.; Li, Y. − C.; Wu, M. C. H.; Mizuse, K.; Kobayashi, T.; Fujii, A.; Kuo, J. − L. Folding of the Hydrogen Bond Network of $H^+(CH_3OH)_7$ with Rare Gas Tagging. *J. Phys. Chem. A* **2013**, *117*, 101−107.
(26) Fifen, J. J.; Nsangou, M.; Dhaouadi, Z.; Motapon, O.; Jaidane, N. − E. Structures of Protonated Methanol Clusters and Temperature Effects. *J. Chem. Phys.* **2013**, *138*, 184301.
(27) Kuo, J. L.; Klein, M. L. Structure of Protonated Water Clusters: Low-Energy Structures and Finite Temperature Behavior. *J. Chem. Phys.* **2005**, *122*, 024516.
(28) Kazimirski, J. K.; Buch, V. Search for Low Energy Structures of Water Clusters $(H_2O)_n$, n = 20−22, 48, 123, and 293. *J. Phys. Chem. A* **2003**, *107*, 9762−9775.
(29) Wu, C. C.; Lin, C. K.; Chang, H. C.; Jiang, J. C.; Kuo, J. L.; Klein, M. L. Protonated Clathrate Cages Enclosing Neutral Water Molecules: $H^+(H_2O)_{21}$ and $H^+(H_2O)_{28}$. *J. Chem. Phys.* **2005**, *122*, 074315.
(30) Jiang, J. C.; Chang, H. C.; Lee, Y. T.; Lin, S. H. Ab initio Studies of $NH_4^+(H_2O)_{1-5}$ and the Influence of Hydrogen-Bonding Non-additivity on Geometries and Vibrations. *J. Phys. Chem. A* **1999**, *103*, 3123−3135.
(31) Khan, A. Theoretical Studies of the Clathrate Structures of $(H_2O)_{20}$, $H^+(H_2O)_{20}$ and $H^+(H_2O)_{21}$. *Chem. Phys. Lett.* **1994**, *217*, 443−450.
(32) Singh, N. J.; Park, M.; Min, S. K.; Suh, S. B.; Kim, K. S. Magic and Antimagic Protonated Water Clusters: Exotic Structures with Unusual Dynamic Effects. *Angew. Chem., Int. Ed.* **2006**, *45*, 3795−3800.
(33) Fridgen, T. D. Structures of Heterogeneous Proton-Bond Dimers with a High Dipole Moment Monomer: Covalent vs Electrostatic Interactions. *J. Phys. Chem. A* **2006**, *110*, 6122−6128.
(34) Rasaiah, J. C.; Garde, S.; Hummer, G. Water in Nonpolar Confinement: From Nanotubes to Proteins and Beyond. *Annu. Rev. Phys. Chem.* **2008**, *59*, 713−740.
(35) Chang, H. − C.; Jiang, J. − C.; Hahndorf, I.; Lin, S. H.; Lee, Y. T.; Chang, H. − C. Migration of an Excess Proton upon Asymmetric Hydration: $H^+[(CH_3)_2O](H_2O)_n$ as a Model System. *J. Am. Chem. Soc.* **1999**, *121*, 4443−4450.
(36) Cheng, T. C.; Bandyopadhyay, B.; Mosley, J. D.; Duncan, M. D. IR Spectroscopy of Protonation in Benzene−Water Nanoclusters: Hydronium, Zundel, and Eigen at a Hydrophobic Interface. *J. Am. Chem. Soc.* **2012**, *134*, 13046−13055.
(37) Bing, D.; Hamashima, T.; Tsai, C. − W.; Fujii, A.; Kuo, J.-L. Proton Location in $(CH_3)_3N$-H^+-$(CH_3OH)_n$: A Theoretical and Infrared Spectroscopic Study. *Chem. Phys.* **2013**, *421*, 1−9.
(38) Shishido, R.; Kuo, J. − L.; Fujii, A. Structures and Dissociation Channels of Protonated Mixed Clusters around a Small Magic Number: Infrared Spectroscopy of $((CH_3)_3N)_n$−H^+−H_2O (n = 1−3). *J. Phys. Chem. A* **2012**, *116*, 6740−6749.
(39) Stace, A. J.; Shukla, A. K. Preferential Solvation of Hydrogen Ions in Mixed Clusters of Water, Methanol, and Ethanol. *J. Am. Chem. Soc.* **1982**, *104*, 5314−5318.
(40) Stace, A. J.; Moore, C. Solvation of Hydrogen Ions in Mixed Water-Alcohol Ion Clusters. *J. Am. Chem. Soc.* **1983**, *105*, 1814−1819.
(41) Deakyne, C. A.; Meot-Ner (Mautner), M.; Campbell, C. L.; Hughes, M. G.; Murphy, S. P. Multicomponent Cluster Ions. I. The Proton Solvated by CH_3CN/H_2O. *J. Chem. Phys.* **1986**, *84*, 4958.
(42) Kebarle, P.; Haynes, R. M.; Collins, J. G. Competitive Solvation of the Hydrogen Ion by Water and Methanol Molecules Studied in the Gas Phase. *J. Am. Chem. Soc.* **1967**, *89*, 5753−5757.
(43) Meot-Ner, M. Multicomponent Cluster Ions. 2. Comparative Stabilities of Cationic and Anionic Hydrogen-Bonded Networks. Mixed Clusters of Water-Methanol. *J. Am. Chem. Soc.* **1986**, *108*, 6189−6197.
(44) Herron, W. J.; Coolbaugh, M. T.; Vaidyanathan, G.; Peifer, W. R.; Garvey, J. F. Observation of Magic Numbers for $(ROH)_nH_3O^+$ Heteroclusters (R = CH_3, CH_3CH_2, $(CH_3)_2CH$, and $CH_3CH_2CH_2$): Implications for Cluster Ion Structure. *J. Am. Chem. Soc.* **1992**, *114*, 3684−3689.

DOI: 10.1021/acs.jpca.7b03762
J. Phys. Chem. A 2017, 121, 5399−5413

(45) Karpas, Z.; Eiceman, G. A.; Harden, C. S.; Ewing, R. G.; Smith, P. B. W. Collision-Induced Dissociation Studies of Protonated Alcohol and Alcohol—Water Clusters by Atmospheric Pressure Ionization Tandem Mass Spectrometry. 1-Methanol. *Org. Mass Spectrom.* **1994**, *29*, 159−168.
(46) Karpas, Z.; Eiceman, G. A.; Ewing, R. G.; Harden, C. S. Collision Induced Dissociation Studies of Protonated Alcohol and Alcohol—Water Clusters by Atmospheric Pressure Ionization Tandem Mass Spectrometry.: Part 2. Ethanol, Propanol and Butanol. *Int. J. Mass Spectrom. Ion Processes* **1994**, *133*, 47−58.
(47) Lyktey, M. M. Y.; DeLeon, R. L.; Shores, K. S.; Furlani, T. R.; Garvey, J. F. Migration of a Proton as a Function of Solvation within $\{ROH\}_n\{H_2O\}H^+$ Cluster Ions: Experiment and Theory. *J. Phys. Chem. A* **2000**, *104*, 5197−5203.
(48) Jackson, P. Tandem Mass Spectrometry Study of Protonated Methanol−Water Aggregates. *Int. J. Mass Spectrom.* **2004**, *232*, 67−77.
(49) Meot-Ner (Mautner), M. The Ionic Hydrogen Bond. *Chem. Rev.* **2005**, *105*, 213−284.
(50) Wei, S.; Tzeng, W. B.; Keesee, R. G.; Castleman, A. W. Metastable Unimolecular and Collision-Induced Dissociation of Hydrogen-Bonded Clusters: Evidence for Intracluster Molecular Rearrangement and the Structure of Solvated Protonated Complexes. *J. Am. Chem. Soc.* **1991**, *113*, 1960−1969.
(51) Wei, S.; Tzeng, W. B.; Castleman, A. W. Structure of Protonated Solvation Complexes: Ammonia-Trimethylamine Cluster Ions and Their Metastable Decompositions. *J. Phys. Chem.* **1991**, *95*, 585−591.
(52) Wu, C. C.; Jiang, J. C.; Boo, D. W.; Lin, S. H.; Lee, Y. T.; Chang, H. C. Behaviors of an Excess Proton in Solute-Containing Water Clusters: A Case Study of $H^+(CH_3OH)(H_2O)_{1-6}$. *J. Chem. Phys.* **2000**, *112*, 176−188.
(53) Chaudhuri, C.; Jiang, J. C.; Wang, X.; Lee, Y. T.; Chang, H. C. Identification of $CH_3OH_2^+$ and H_3O^+-Centered Cluster Isomers from Fragment-Dependent Vibrational Predissociation Spectra of $H^+(CH_3OH)_4H_2O$. *J. Chem. Phys.* **2000**, *112*, 7279−7282.
(54) Jiang, J. C.; Chaudhuri, C.; Lee, Y. T.; Chang, H. C. Hydrogen Bond Rearrangements and Interconversions of $H^+(CH_3OH)_4H_2O$ Cluster Isomers. *J. Phys. Chem. A* **2002**, *106*, 10937−10944.
(55) Wu, C. C.; Chaudhuri, C.; Jiang, J. C.; Lee, Y. T.; Chang, H. − C. Structural Isomerism and Competitive Proton Solvation between Methanol and Water in $H^+(CH_3OH)_m(H_2O)_n$, $m + n = 4$. *J. Phys. Chem. A* **2004**, *108*, 2859−2866.
(56) Suhara, K.; Fujii, A.; Mizuse, K.; Mikami, N.; Kuo, J. − L. Compatibility between Methanol and Water in the Three-Dimensional Cage Formation of Large-Sized Protonated Methanol-Water Mixed Clusters. *J. Chem. Phys.* **2007**, *126*, 194306.
(57) Kuo, J. − L.; Xie, Z. − Z.; Bing, D.; Fujii, A.; Hamashima, T.; Suhara, K.; Mikami, N. Comprehensive Analysis of the Hydrogen Bond Network Morphology and OH Stretching Vibrations in Protonated Methanol-Water Mixed Clusters, $H^+(MeOH)_1(H2O)_n$ (n = 1−8). *J. Phys. Chem. A* **2008**, *112*, 10125−10133.
(58) Bing, D.; Kuo, J. − L.; Suhara, K.; Fujii, A.; Mikami, N. Proton Switch Correlated with the Morphological Development of the Hydrogen-Bond Network in $H^+(MeOH)_m(H_2O)_1$ (m = 1−9): A Theoretical and Infrared Spectroscopic Study. *J. Phys. Chem. A* **2009**, *113*, 2323−2332.
(59) Bing, D.; Hamashima, T.; Nguyen, Q. C.; Fujii, A.; Kuo, J. − L. Comprehensive Analysis on the Structure and Proton Switch in $H^+(CH_3OH)_m(H_2O)_n$ ($m + n$ = 5 and 6). *J. Phys. Chem. A* **2010**, *114*, 3096−3102.
(60) Bing, D.; Hamashima, T.; Fujii, A.; Kuo, J. − L. Anticooperative Effect Induced by Mixed Solvation in $H^+(CH_3OH)_m(H_2O)_n$ ($m + n$ = 5 and 6): A Theoretical and Infrared Spectroscopic Study. *J. Phys. Chem. A* **2010**, *114*, 8170−8177.
(61) Ryding, M. J.; Izsák, R.; Merlot, P.; Reine, S.; Helgaker, T.; Uggerud, E. Geometry of the Magic Number $H^+(H_2O)_{21}$ Water Cluster by Proxy. *Phys. Chem. Chem. Phys.* **2015**, *17*, 5466−5473.
(62) Hunter, E. P.; Lias, S. G. Evaluated Gas Phase Basicities and Proton Affinities of Molecules: An Update. *J. Phys. Chem. Ref. Data* **1998**, *27*, 413−457.
(63) Okumura, M.; Yeh, L. I.; Myers, J. D.; Lee, Y. T. Infrared Spectra of the Cluster Ions $H_7O_3^+ \cdot H_2$ and $H_9O_4^+ \cdot H_2$. *J. Chem. Phys.* **1986**, *85*, 2328−2329.
(64) Okumura, M.; Yeh, L. I.; Myers, J. D.; Lee, Y. T. Infrared Spectra of the Solvated Hydronium Ion: Vibrational Predissociation Spectroscopy of Mass-Selected $H_3O^+ \cdot (H_2O)_n \cdot (H_2)_m$. *J. Phys. Chem.* **1990**, *94*, 3416−3427.
(65) Mizuse, K.; Fujii, A. Infrared Photodissociation Spectroscopy of $H^+(H_2O)_6 \cdot M_m$ (M = Ne, Ar, Kr, Xe, H_2, N_2, and CH_4): Messenger-Dependent Balance between H_3O^+ and $H_5O_2^+$ Core Isomers. *Phys. Chem. Chem. Phys.* **2011**, *13*, 7129−7135.
(66) Kuo, J. L.; Klein, M. L. Structure of Protonated Water Clusters: Low-Energy Structures and Finite Temperature Behavior. *J. Chem. Phys.* **2005**, *122*, 024516.
(67) Nguyen, Q. C.; Ong, Y. S.; Soh, H.; Kuo, J. − L. Multiscale Approach to Explore the Potential Energy Surface of Water Clusters $(H_2O)_n$ $n \leq 8$. *J. Phys. Chem. A* **2008**, *112*, 6257−6261.
(68) Nguyen, Q. C.; Ong, Y. − S.; Kuo, J. − L. A Hierarchical Approach to Study the Thermal Behavior of Protonated Water Clusters $H^+(H_2O)_n$. *J. Chem. Theory Comput.* **2009**, *5*, 2629−2639.
(69) Even, U.; Jortner, J.; Noy, D.; Lavie, N.; Cossart-Magos, C. Cooling of Large Molecules below 1 K and He Clusters Formation. *J. Chem. Phys.* **2000**, *112*, 8068−8071.
(70) Zhang, X.; Yang, X.; Castleman, A. W., Jr. Study of Protonated Methanol Cluster Ions under Thermal Conditions. *Chem. Phys. Lett.* **1991**, *185*, 298−302.
(71) Lu, E. − P.; Pan, P. − R.; Li, Y. − C.; Tsai, M. − K.; Kuo, J. − L. Structural Evolution and Solvation of the OH Radical in Ionized Water Radical Cations $(H_2O)_n^+$, n = 5−8. *Phys. Chem. Chem. Phys.* **2014**, *16*, 18888−18895.
(72) Lin, R. − J.; Nguyen, Q. C.; Ong, Y. − S.; Takahashi, K.; Kuo, J. − L. Temperature Dependent Structural Vibrations of $OH^-(H_2O)_n$, n = 4−7: Effects on Vibrational and Photoelectron Spectra. *Phys. Chem. Chem. Phys.* **2015**, *17*, 19162−19172.
(73) Wales, D. J.; Scheraga, H. A. Global Optimization of Clusters, Crystals, and Biomolecules. *Science* **1999**, *285*, 1368−1372.
(74) Ojamäe, L.; Shavitt, I.; Singer, S. J. Potential Models for Simulations of the Solvated Proton in Water. *J. Chem. Phys.* **1998**, *109*, 5547−5564.
(75) Frisch, M. J.; Trucks, G. W.; Schlegel, H. B.; Scuseria, G. E.; Robb, M. A.; Cheeseman, J. R.; Scalmani, G.; Barone, V.; Mennucci, B.; Petersson, G. A.; et al. *Gaussian 09*, Revision E.01;Gaussian, Inc.::Wallingford CT, 2009.
(76) Wales, D. J.; Ohmine, I. Structure, Dynamics, and Thermodynamics of Model $(H_2O)_8$ and $(H_2O)_{20}$ Clusters. *J. Chem. Phys.* **1993**, *98*, 7245−7256.
(77) Calvo, F.; Doye, J. P. K.; Wales, D. J. Equilibrium Properties of Clusters in the Harmonic Superposition Approximation. *Chem. Phys. Lett.* **2002**, *366*, 176−183.
(78) Bogdan, T. V.; Wales, D. J.; Calvo, F. Equilibrium Thermodynamics from Basin-Sampling. *J. Chem. Phys.* **2006**, *124*, 044102.
(79) Wang, Y. − S.; Jiang, J. − C.; Cheng, C. − L.; Lin, S. − H.; Lee, Y. − T.; Chang, H. − C. Identifying 2- and 3-coordinated H_2O in Protonated Ion−water Clusters by Vibrational Pre-dissociation Spectroscopy and *ab initio* Calculations. *J. Chem. Phys.* **1997**, *107*, 9695−9698.
(80) Kobayashi, T.; Shishido, R.; Mizuse, K.; Fujii, A.; Kuo, J. − L. Structures of Hydrogen Bond Networks Formed by a Few Tens of Methanol Molecules in the Gas Phase: Size-selective Infrared Spectroscopy of Neutral and Protonated Methanol Clusters. *Phys. Chem. Chem. Phys.* **2013**, *15*, 9523−9530.
(81) Cheng, Y. − L.; Chen, H. − Y.; Takahashi, K. Theoretical Calculation of the OH Vibrational Overtone Spectra of 1-*n* Alkane Diols (n = 2−4): Origin of Disappearing Hydrogen-Bonded OH Peak. *J. Phys. Chem. A* **2011**, *115*, 5641−5653.
(82) Morita, M.; Takahashi, K. Theoretical Study on the Difference of OH Vibrational Spectra between $OH^-(H_2O)_3$ and $OH^-(H_2O)_4$. *Phys. Chem. Chem. Phys.* **2012**, *14*, 2797−808.

DOI: 10.1021/acs.jpca.7b03762
J. Phys. Chem. A 2017, 121, 5399−5413

(83) Wang, Y. − S.; Tsai, C. − H.; Lee, Y. T.; Chang, H. − C.; Jiang, J. C.; Asvany, O.; Schlemmer, S.; Gerlich, D. Investigations of Protonated and Deprotonated Water Clusters Using a Low-Temperature 22-Pole Ion Trap. *J. Phys. Chem. A* **2003**, *107*, 4217−4225.
(84) Shimamori, T.; Kuo, J. − L.; Fujii, A. Stepwise Internal Energy Change of Protonated Methanol Clusters By Using the Inert Gas Tagging. *J. Phys. Chem. A* **2016**, *120*, 9203−9208.
(85) Malloum, A.; Fifen, J. J.; Dhaouadi, Z.; Engo, S. G. N.; Jaidane, N. − E. Structures and Relative Stabilities of Ammonia Clusters at Different Temperatures: DFT vs. ab initio. *Phys. Chem. Chem. Phys.* **2015**, *17*, 29226−29242.
(86) Malloum, A.; Fifen, J. J.; Dhaouadi, Z.; Nana Engo, S. G.; Jaidane, N.-E. Structures and Spectroscopy of Medium Size Protonated Ammonia Clusters at Different Temperatures, $H^+(NH_3)_{10-16}$. *J. Chem. Phys.* **2017**, *146*, 044305.
(87) Ishikawa, H.; Kurusu, I.; Yagi, R.; Kato, R.; Kasahara, Y. Quantitative Temperature Dependence of the Microscopic Hydration Structures Investigated by Ultraviolet Photodissociation Spectroscopy of Hydrated Phenol Cations. *J. Phys. Chem. Lett.* **2017**, *8*, 2541−2546.
(88) Rodriguez, O., Jr.; Lisy, J. M. Revisiting $Li^+(H_2O)_{3-4}Ar_1$ Clusters: Evidence of High-Energy Conformers from Infrared Spectra. *J. Phys. Chem. Lett.* **2011**, *2*, 1444−1448.

DOI: 10.1021/acs.jpca.7b03762
J. Phys. Chem. A 2017, 121, 5399−5413